

GA-A25445

TARGET PLATE CONDITIONS DURING STOCHASTIC BOUNDARY OPERATION ON DIII-D

by

**J.G. WATKINS, T.E. EVANS, C.J. LASNIER,
R.A. MOYER, and D.L. RUDAKOV**

JUNE 2006



DISCLAIMER

This report was prepared as an account of work sponsored by an agency of the United States Government. Neither the United States Government nor any agency thereof, nor any of their employees, makes any warranty, express or implied, or assumes any legal liability or responsibility for the accuracy, completeness, or usefulness of any information, apparatus, product, or process disclosed, or represents that its use would not infringe privately owned rights. Reference herein to any specific commercial product, process, or service by trade name, trademark, manufacturer, or otherwise, does not necessarily constitute or imply its endorsement, recommendation, or favoring by the United States Government or any agency thereof. The views and opinions of authors expressed herein do not necessarily state or reflect those of the United States Government or any agency thereof.

TARGET PLATE CONDITIONS DURING STOCHASTIC BOUNDARY OPERATION ON DIII-D

by

J.G. WATKINS,* T.E. EVANS, C.J. LASNIER,†
R.A. MOYER,‡ and D.L. RUDAKOV‡

This is a preprint of a paper to be presented at
the 17th International Conference on Plasma
Surface Interactions in Controlled Fusion
Devices, Hefei, China, May 22–26, 2006 and to be
printed in the Proceedings.

*Sandia National Laboratories, Albuquerque, New Mexico

†Lawrence Livermore National Laboratory, Livermore, California, USA

‡University of California San Diego, La Jolla, California

Work supported by
the U.S. Department of Energy
under DE-FC02-04ER54698, DE-AC04-94AL85000,
DE-FG02-04ER54758, and W-7405-ENG-48

GENERAL ATOMICS PROJECT 30200
JUNE 2006



ABSTRACT

A major concern for large tokamaks like ITER is the presence of edge localized modes (ELMs) that repeatedly send large bursts of particles and heat into the divertor plates. Operation with resonant magnetic perturbations (RMP) at the boundary of DIII-D has suppressed ELMs for values of $q_{95} \sim 3.7$. At the target plate, the conditions during ELM-suppressed operation for both high and low collisionality are observed by a set of radially distributed Langmuir probes. At high collisionality ($\nu_e^* \sim 1$), the target plate particle flux and temperature drop by > 30% during ELM suppression. At low collisionality ($\nu_e^* \sim 1$), the core density, target plate density, and target plate particle flux drop but the plate electron temperature increases after the ELMs are suppressed. The ELM-suppressed target plate heat flux is nearly the same as the heat flux between ELMs but the (5x higher) transient heat flux peaks due to ELMs are eliminated.

1. INTRODUCTION

Unacceptable erosion and thermal loading of the divertor plates are predicted [1,2] for Type 1 ELMing H-mode operation in large tokamaks like ITER. One possible solution has been recently demonstrated [3-7] in DIII-D operation with resonant magnetic perturbations (RMP) at the boundary. These plasmas exhibit ELM suppression [Fig. 1(a,b)] over a range of pedestal electron collisionalities $0.1 < \nu_e^* < 1.0$ [Fig. 1(c)] while maintaining high energy confinement as indicated by the H-mode confinement quality factor H [Fig. 1(d)]. At the low end of the ν_e^* range ($\nu_e^* \sim 0.1$), the ELM suppression is achieved at pedestal electron collisionalities expected for ITER. This magnetically perturbed boundary is produced by a special set of coils (I-coils [8]) that generate small resonant perturbations of the edge magnetic field. The RMPs and ELM suppression effects exhibit a resonance behavior centered around an edge q value at the $\psi_n = 0.95$ flux surface of $q_{95} = 3.7$, where ψ_n is the poloidal magnetic flux normalized to the value on the separatrix (an effective radial coordinate in non-circular plasmas). At the target plate, the conditions during ELM-suppressed operation are observed with a radial array of Langmuir probes for both high and low collisionality cases.

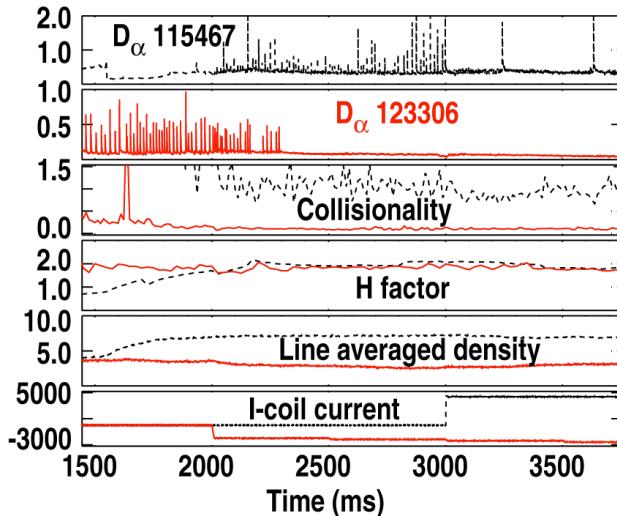


Fig. 1. The dashed line shows the high collisionality ELM suppression case. The low collisionality case (solid) is similar to ITER pedestal collisionality and is achieved with a larger magnetic perturbation using even parity. This case also had more effective ELM suppression, lower pedestal density and higher target plate temperatures.

2. EXPERIMENTAL SETUP

Double-null plasma discharges with high triangularity (high density, high collisionality, magnetically shifted slightly down) and lower single null plasmas with low triangularity (low density, low collisionality) were used for these experiments. The low collisionality case was obtained by pumping with the lower divertor cryopump, which required a low triangularity shape to place the outer strike point near the pump entrance. In these experiments, the ion $B \times \nabla B$ drift was directed toward the main (lower) divertor. Both cases have similar edge q but have different densities. The edge q was varied by changing the plasma current.

The resonant magnetic perturbation at the boundary was generated using an installed set of rectangular or “window pane” coils internal to the DIII-D vacuum vessel. These coils are mounted under the outer wall graphite tiles and were energized with up to 4.5 kA of current during plasma discharges. Target plate measurements were made during and after the transition to the ELM-suppressed regime using a fixed radial array of Langmuir probes [9,10]. The probe voltage sweeping was at 1250 Hz to improve time resolution and accuracy during ELMs and oscillations.

3. OBSERVATIONS

3.1. HIGH COLLISIONALITY

At high collisionality ($\nu^* \sim 1$) and q_{95} fixed near optimum comparing characteristic values when the perturbation coil is energized to the value between ELMs, the target plate particle flux drops by 30%, the temperature drops by 50%, and the probe floating potential (V_f) goes to approximately zero across the floor. These changes indicate that the plasma is tending toward detachment. Also at high collisionality, small oscillations near the ELM frequency but with amplitude clamped at a value much smaller than the ELM level are observed in temperature, density, and H_α at the target plate after the ELMs are suppressed (Fig. 2). The ELM peak heat flux is reduced by a factor of at least 5 at the divertor plates as measured by the infrared camera [4].

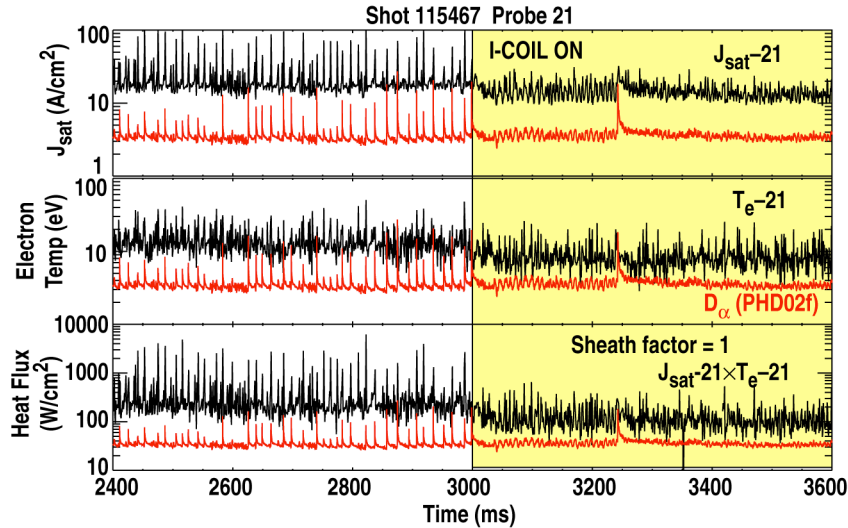


Fig. 2. High Collisionality target plate conditions during ELM suppression using the resonant magnetic perturbation (RMP). Particle flux and temperature at $R_{sep} + 2$ cm are compared before and after the transition. The baseline level of particle flux drops 30% and the baseline level of electron temperature drops 50% when the coil is energized. Small oscillations are seen in target plate density and temperature as well as H_α light after the transition but only last until the first large ELM.

The peak particle flux measured during an ELM before the RMP is energized drops by a factor of ~ 10 after the RMP is energized and the ELMs are suppressed. Figure 2 shows the time window when the RMP is energized and shows that, 2 cm outboard of the outer strike point, the temperature and the particle flux drop when the RMP is energized. For these cases with conditions near optimum for ELM suppression, the target plate electron temperature (baseline/between ELMs) is observed to drop by 30% to 50% within 20 ms after the perturbation coils are energized. The target plate particle flux (between ELMs) decreases by 30% when the coil is energized.

The floating potentials measured at three divertor plate locations change when the coils are energized. Three V_f measurements were at 2, 5, and 8 cm beyond the outer strikepoint. Two of these measurements (5 and 8 cm) reduce to zero at the transition when the RMP coils are energized. This is an indication that the temperature has decreased in the outer SOL and that there is little sheath acceleration of ions into the plate in this region. This is consistent with lower levels of heat flux at the plates.

Resonant behavior in q_{95} is observed in the target plate conditions as well as in the effectiveness of the RMP to suppress ELMs. The time history of the q scan can be seen in Fig. 3. The ELM suppression q window is shown in the particle flux contour plot measured at the lower divertor plate. The D_α signal measured in the same region (FS03) is shown for reference. During a scan of q_{95} , obtained by ramping up I_p during RMP operation, Fig. 4 shows the between ELM target plate particle flux is maximized and the target plate electron temperature is minimized at $q_{95}=3.7$, the same resonant value required for optimum ELM suppression. The edge q dependence of the electron temperature and density can also be seen in Fig. 4. The q window for ELM suppression can be seen in the signals in Fig. 4 near $q_{95} = 3.7$.

Unique oscillations are observed at the target plate during ELM-suppressed RMP operation. The oscillations first appear about 50 ms after the start of the I-coil pulse at 3000 ms into the discharge and can be seen on the divertor D_α as well as the target plate flux and temperature as shown in Fig. 2. The oscillations in particle flux and temperature measured by the Langmuir probes increase and then decrease together in time. A detailed discussion of the oscillations and the core plasma can be found elsewhere [7].

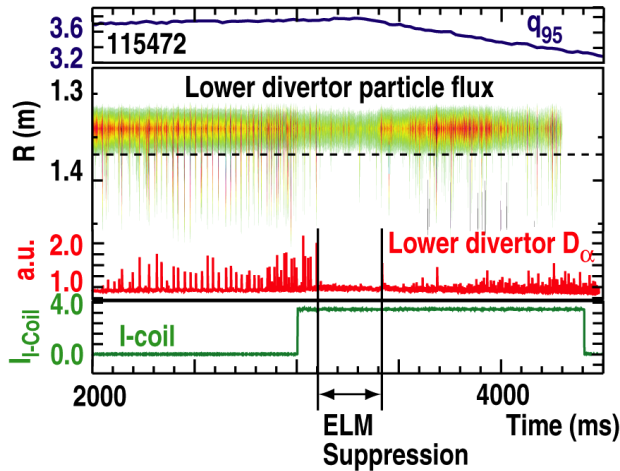


Fig. 3. The figure shows a contour plot ($\nu_e^* \sim 1$) of the target plate particle flux during the q scan. The vertical axis is major radius and the horizontal axis is time for all the traces. The RMP is energized at 3000 ms (bottom trace versus time) and the ELM suppression is seen where the edge q is within the suppression window (around 3.7). Several events can be seen later in the discharge when q decreases out of the resonant window.

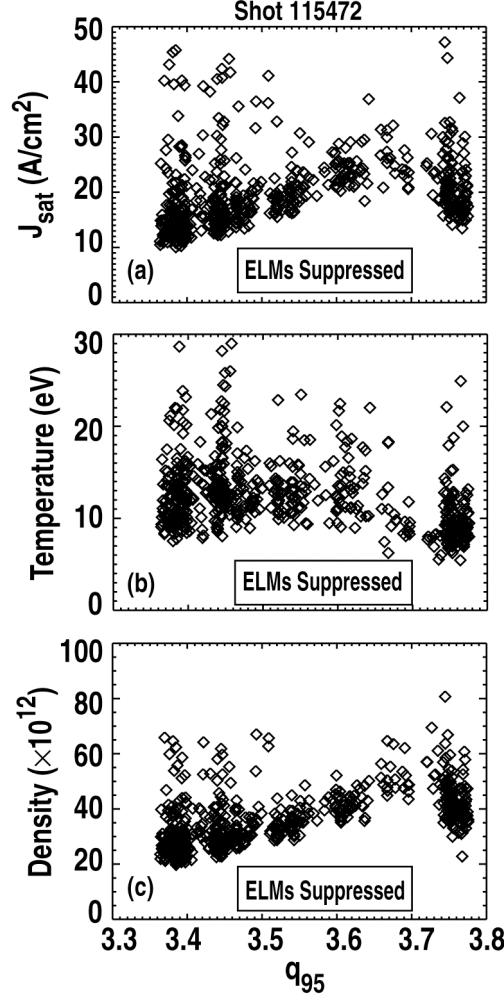


Fig. 4. Conditions at the target plate 2 cm outboard of the outer strikepoint ($v_e^* \sim 1$) are shown as a function of edge q . The ELM suppression can be seen in a window around $q_{95} = 3.7$. The maximum target plate particle flux and minimum target plate electron temperature occur near the q value for optimum ELM suppression. This implies that the amplitude of the magnetic perturbation and the enhanced radial transport are also maximized for this q .

3.2. LOW COLLISIONALITY

In low collisionality plasmas ($\nu^* \sim 0.1$), after the ELMs are suppressed, the core density drops, the target plate particle flux drops by 25% while the electron temperature at the plate increases by about 100%. We observe the floating potential at the strike point ($R_{probe} = R_{strike} + 0.1$ cm) drop strongly after the ELMs are suppressed to -150 V as seen in Fig. 5. The perpendicular heat flux during the ELM-suppressed phase is about 15 W/cm 2 between ELMs before the RMP is applied and 20 W/cm 2 after ELMs are suppressed. The Langmuir probe heat flux agrees with the IR camera if a sheath factor of 1 is used as shown in Fig. 6. So the background heat flux does not change much after the I-coil is energized but

the transient heat flux peaks due to ELMs (5x higher than between ELMs) are eliminated. No oscillations of the type seen in high collisionality are observed.

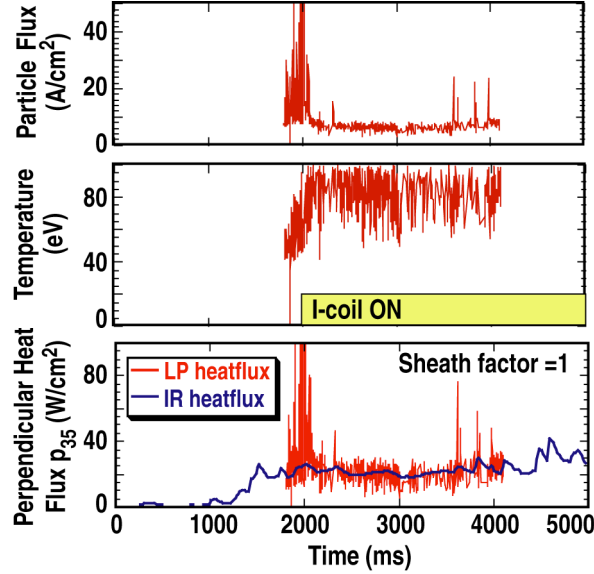


Fig. 5. At low collisionality, the floating potential goes very negative when the ELMs go away. This is consistent with hot electrons hitting the target plate.

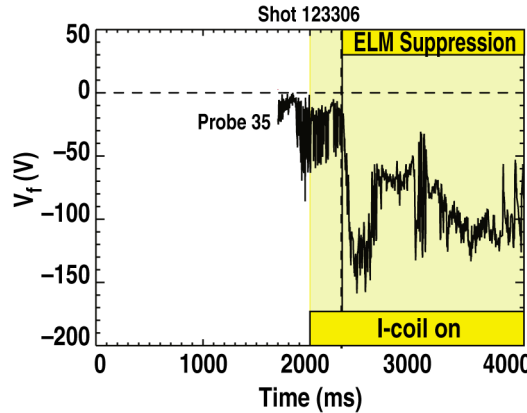


Fig. 6. Low collisionality target plate conditions are shown for a Langmuir probe near the strike point ($R_{strike} + 0.1$ cm). The electron temperature goes up and the target plate flux goes down when the coil is energized at 2000 ms. The ELMs go away at 2350 ms. Using a sheath factor = 1 to get LP heat flux ($q = \delta\Gamma \times T_e$) to agree with the IR camera is typical for the strike point at DIII-D.

4. DISCUSSION

4.1 HIGH COLLISIONALITY

During RMP operation at high collisionality, the peak values (in time) of the particle flux and temperature at the target plate drop significantly because of the disappearance of most of the ELMs. Additionally, the baseline particle flux and temperature after the start of the I-coil pulse decrease and the floating potential drops to zero. We expected to lower the divertor temperature and density by distributing heat and particle flux from the strike point over a larger area due to the modifications in the flux surface geometry and enhanced radial transport. The 30% drop in particle flux and 50% drop in temperature imply that the baseline heat flux at the probe location during ELM suppression should be about four times lower than the heat flux measured between ELMs before the RMP is energized. The temperature reaches a minimum when the edge q is adjusted to maximize the particle flux. This should also minimize the steady state heat flux. These trends are leading toward divertor detachment if not already achieved. More detailed profiles with data closer to the strike point are needed to determine if this is the case. Even at 2 cm into the SOL, we see the temperature drop to less than 5 eV. The oscillations, which appear at the target plate after the ELMs are suppressed, are related to bursts in magnetic and electrostatic fluctuations in the pedestal that then lead to enhanced transport [7]. The oscillations have a longer duration and slower rise time than the ELMs but the integral of the particle flux is about the same as during the ELMs thus the particle and heat impulse are substantially reduced due to the longer period of the oscillations. It is the high impulse that is predicted for ITER-like ELMs that erodes or ablates particles.

4.2. LOW COLLISIONALITY

At low collisionality, more typical of ITER conditions, the observation of higher baseline electron temperature at the target plate is typical of lower density operation where radiation losses are smaller in the divertor because of reduced recycling. The very large negative floating potential measured when the ELMs are suppressed also indicates the presence of high temperature electrons from the upstream SOL (low density, low recycling divertor). These hot electrons may possibly come from deep inside the steep pedestal plasma gradient region. Field line tracing calculations [11] predict that a few percent of the core field lines wander out of the core and into the target plate for larger magnetic perturbations as were used in the low collisionality ELM suppression cases. Even a small population of hot electrons at the target can significantly modify the sheath potential for ion acceleration and enhance sputtering of carbon [12].

5. CONCLUSIONS

RMP operation, by suppressing ELMs and significantly reducing heat and particle fluxes at the target plates, greatly improves the outlook for operating large H-mode fusion reactors. The high collisionality experiments described here show that the baseline levels of particle flux and electron temperature drop after the transition and depend on the edge q . The maximum particle flux and minimum temperature occur at the optimum q for ELM suppression and imply that this q is where the perturbations have the most effect. By applying the RMPs at low collisionality, the impulsive heat loading during ELMs has been converted to a more steady-state heat loading which keeps the peak heat flux below the expected ITER ablation limit.

In the future, we plan to explore details of the edge RMP effects on the target plate flux and temperature profiles with a new higher spatial resolution probe array.

REFERENCES

- [1] A.W. Leonard, et al., *J. Nucl. Mater.* **266–269** (1999) 109.
- [2] A.W. Leonard, et al., *Phys. Plasmas* **10** (2003) 1765.
- [3] T.E. Evans, R. Moyer, P. Thomas, J.G. Watkins, et al., *Phys. Rev. Lett.* **92** (2004) 235003-1.
- [4] T.E. Evans, R.A. Moyer, J.G. Watkins, et al., *Nucl. Fusion* **45** (2005) 595.
- [5] T. Evans, *J. Nucl. Mater.* **1–2** (1993) 160.
- [6] K. Burrell, et al., *Plasma Phys. and Controlled Fusion* **47** (2005) B37.
- [7] R.A. Moyer, et al., *Phys. Plasmas* **12** (2005) 056119.
- [8] G.L. Jackson, P.M. Anderson, J. Bialek at al., Proc. 30th European Physical Society Conf. on Controlled Fusion and Plasma Physics, St. Petersburg, Russia 2003, edited by R. Koch and S. Lebedev (European Physical Society, Geneva, 2003), CD-ROM, Paper P-4.47.
- [9] J. Watkins, et al., *J. Nucl. Mater.* **241–243** (1997) 645.
- [10] D. Buchenauer, et al. *Rev. Sci. Instrum.* **61** (1990) 2873.
- [11] L.W. Yan, T.E. Evans, “Modeling of Large ELM Suppression for High Confinement Plasma in DIII-D,” to be presented at the 17th Intl. Conf. on Plasma Surface Interactions in Controlled Fusion Devices, Hefei, China, 2006.
- [12] M.E. Fenstermacher, et al, “Pedestal, SOL, and Divertor Plasma Properties in DIII-D RMP Elm Suppressed Discharges at ITER Relevant Edge Collisionality”, to be presented at the 17th Intl. Conf. on Plasma Surface Interactions in Controlled Fusion Devices, Hefei, China, 2006.

ACKNOWLEDGMENTS

Work supported by the U.S. Department of Energy under Contract Nos. DE-AC04-94AL85000, DE-FC03-04ER54698, DE-FG02-04ER54758, and W-7405-ENG-48.